ASILOMAR 32ND CONFERENCE ON 'SIGNALS, SYSTEMS AND COMPUTERS', MONTEREY 1998

A Simple Statistical Analysis of Wavelet-based Multifractal Spectrum Estimation

Paulo Gonçalvès
INRIA Rocquencourt, Domaine de Voluceau
B.P. 105, 78153 Le Chesnay cedex, France

Rudolf Riedi and *Richard Baraniuk* *
Department of Electrical and Computer Engineering, Rice University
Houston, Texas 77005, USA

Abstract

The multifractal spectrum characterizes the scaling and singularity structures of signals and proves useful in numerous applications, from network traffic analysis to turbulence. Of great concern is the estimation of the spectrum from a finite data record. In this paper, we derive asymptotic expressions for the bias and variance of a wavelet-based estimator for a fractional Brownian motion (fBm) process. Numerous numerical simulations demonstrate the accuracy and utility of our results.

1 Introduction

The study of fractal quantities and structures has proved to be of outstanding significance in many disciplines [2, 9, 12, 13, 14]. The fractional Brownian motion (fBm) random process, for example, has a "fractal" or highly erratic appearance that has proved useful for network traffic, turbulence, and texture modeling.

However, for many applications, fBm is too homogeneous, or monofractal. That is, its local degree of Hölder continuity H_t is the same at all times t. Most real-world signals, on the other hand, exhibit *multifractal* structure, meaning that H_t varies erratically with time [13].

The multifractal structure of a process is efficiently represented by the *multifractal spectrum* $f(a)$, the dimension of the set of times t with $H_t = a$: the smaller $f(a)$ the smaller the chance of finding $H_t = a$. The *multifractal formalism* conveniently relates f to the rate function of a Large Deviation Principle that is very amenable to estimation in practice.

This paper deals with the estimation of the multifractal spectrum from a finite-length, discrete-time data sequence. Since we are interested in the fractal or scaling structure of the sequence, it is no surprise that the multi-scale analysis of the wavelet transform [3] proves convenient. In contrast to previous works on multifractal spectrum estimation, we derive asymptotic expressions for the bias and variance of the estimator (for the case of an fBm analysis). In this way, our work is an extension of that in [1, 4].

*Supported by NSF, grant MIP–9457438, DARPA/AFOSR, grant F49620–97–1–0513, Texas Instruments, and the Rice Consortium for Computational Seismic Interpretation.

Email: paulo.goncalves@inria.fr, riedi@rice.edu, richb@rice.edu
URL: www.dsp.rice.edu

2 Multifractal Analysis

Processes with local singularities (cusps, ridges, edges, chirps, etc.) appear in many fields of endeavor [2, 9, 12, 14]. The singularity behavior of a process $Y(t)$ at time t can be characterized by its Hölder exponent H_t through a comparison with an algebraic function. We define H_t as the largest h such that there exists a polynomial P satisfying $|Y(s) - P(s)| \leq C|s-t|^h$ for s sufficiently close to t.

The *multifractal spectrum* gives a description of the singularity content of a process. In this section, we will overview the 1-d multifractal spectrum theory from the standpoint of wavelet-based estimators.

2.1 Wavelets: Detecting local singularities

The wavelet decomposition conveys information on the oscillatory behavior of a process Y. Consider a 1-d orthogonal, L^1-normalized wavelet basis comprised of elements $\psi_{j,k} := 2^{-j}\psi(2^{-j}t - k)$ with $(j,k) \in \mathsf{Z}^2$ [3]. Assume that the mother wavelet ψ has $\mathcal{R}$ vanishing moments; that is $\int x^r\, \psi(x)\, dx = 0,\ \ r = 0, \ldots, \mathcal{R}$. The L^1-normalized wavelet coefficients of Y are given by

$$d_{j,k} := \int_{-\infty}^{\infty} Y(t)\, 2^{-j}\, \psi(2^{-j}t - k)\, \mathrm{d}t. \qquad (1)$$

Let $k2^j \to t$ mean that $t \in [k2^j, (k+1)2^j[$ and $j \to -\infty$. The argument of [10, p. 291] generalizes easily to show that $|Y(s) - Y(t)| = O(|s-t|^\alpha)$ implies

$$|d_{j,k}| = O(2^{j\alpha}) \qquad \text{as } k2^j \to t. \qquad (2)$$

for any $\alpha > 0$ and any wavelet with $\mathcal{R} > H$. Thus, the oscillatory/scaling behavior of a process carries over into the local scaling properties of its wavelets coefficients, provided the wavelet is more regular than the process.

2.2 Multifractal spectrum

Rather than the Hölder exponent H_t, consider the following wavelet-based *local singularity strength measure*

$$\alpha(t) := \lim_{k2^j \to t} \frac{1}{j} \log_2 |d_{j,k}|\,. \qquad (3)$$

Smaller $\alpha(t)$ correspond to larger oscillations in Y and thus more singular Y at time t. Typically, a process will possess many different singularity strengths. The frequency (in t) of occurrence of a given singularity strength α is measured by the *multifractal spectrum* [15, 14]

$$\begin{aligned} f(\alpha) &:= \lim_{\varepsilon\to 0}\lim_{j\to -\infty} -\frac{1}{j}\log_2 M_j \qquad (4)\\ M_j &:= 2^j \# \left\{k \,:\, 2^{j(\alpha+\varepsilon)} \le |d_{j,k}| \le 2^{j(\alpha-\varepsilon)}\right\}. \end{aligned}$$

For k lying in $0,\ldots,2^{-j}-1$, f takes values between -1 and 0. Smaller $f(\alpha)$ means that "fewer" points t behave with strength $\alpha(t)\simeq\alpha$. If α_0 denotes the value $\alpha(t)$ assumed by "most" points t, then $f(\alpha_0)=0$.

2.3 Multifractal formalism

While the multifractal spectrum f contains valuable information on the singularity behavior of Y, it is, unfortunately, hard to calculate. A simpler approach makes use of the theory of large deviations [5]. In this analysis, f is interpreted as the rate function of a Large Deviation Principle: f measures how frequently (in k) the observed $(1/j)\log|d_{j,k}|$ deviate from the "expected value" α_0 in scale j. In our context, this corresponds to studying the scaling behavior of the moments of the wavelet coefficients (compare also with [2]).

Define the *partition function*

$$T(q) := \lim_{j\to-\infty}\log_2 \mathbb{E}|d_{j,k}|^q. \qquad (5)$$

The partition function measures the scaling of the moments and higher-order dependencies of the wavelet coefficients and the singularity structure of the process all in one. Note that T is always concave, since moment generating functions are log-convex.

The *multifractal formalism* posits that the multifractal spectrum can be calculated by taking the Legendre transform of the corresponding log moment generating function [14, 15]

$$f(\alpha) = f_{\mathrm{L}}(\alpha) := \inf_q[q\alpha - T(q)]. \qquad (6)$$

Simple calculus shows that $f_{\mathrm{L}}(\alpha) = q\alpha - T(q)$ at $\alpha = T'(q)$ provided $T''(q)<0$. For obvious reasons, the function $f_{\mathrm{L}}(\alpha)$ is termed the *Legendre spectrum.*

2.4 Fractional Brownian motion

A fractional Brownian motion (fBm) B with parameter H is a non-stationary Gaussian process $B(t)\sim N(0,\sigma^2|t|^{2H})$ with stationary self-similar increments [6]

$$B(t+\tau)-B(t) \stackrel{d}{=} B(\tau)-B(0) \stackrel{d}{=} \tau^H B(1). \qquad (7)$$

(Here $\stackrel{d}{=}$ denotes equality in finite-dimensional distribution.) The wavelet coefficients of an fBm sport the following properties [6]

P1. stationarity: $d_{j,k} \stackrel{d}{=} d_{j,0} \quad \forall\, k.$

P2. Gaussianity: $d_{j,k}\sim N(0,\sigma_\psi 2^{2jH})$, with σ_ψ a constant depending on ψ.

P3. almost decorrelation: $\mathbb{E}[d_{j,k}d_{j',k'}] \simeq |2^{-j}k - 2^{-j'}k'|^{2(H-\mathcal{R})}$.

P4. scaling: $d_{j,k} \stackrel{d}{=} 2^{jH}\, d_{0,k}$.

Because of P2 and P3, we will assume henceforth that the fBm wavelet coefficients are exactly uncorrelated and hence independent. This is not an unreasonable assumption [6]. Furthermore, since the moments of order $q\le -1$ of a Gaussian are infinite, either P2 or P4 yields

$$T(q) = \begin{cases} qH & q>-1 \\ -\infty & q\le -1\end{cases} \qquad (8)$$

and thus that

$$f(\alpha) = f_{\mathrm{L}}(\alpha) = \begin{cases} -\infty & \alpha<H \\ 0 & \alpha = H \\ H-\alpha & \alpha>H\end{cases} \qquad (9)$$

3 Multifractal Spectrum Estimation using Wavelets

We now discuss wavelet-based estimation of the multifractal spectrum. In the simple case of fBm, we will derive asymptotic results on the first and second order statistics of the estimate.

3.1 Wavelet-based estimator

To estimate the multifractal spectrum given N samples of a single realization of an fBm process, we take advantage of the stationarity of the wavelet coefficients $\{d_{j,k} \,:\, j = 1,\ldots,\log_2(N),\, k=0,\ldots,N2^{-j}-1\}$ within scale. For $q>-1$, define the crude sample estimator for the moments of the wavelet coefficients as follows:[1]

$$\begin{aligned} \widehat{S}_j(q) &:= \frac{1}{N2^{-j}}\sum_{k=0}^{N2^{-j}-1}|d_{j,k}|^q \qquad (10)\\ &\stackrel{d}{=} 2^{jqH}\frac{1}{N2^{-j}}\sum_{k=0}^{N2^{-j}-1}|d_{0,k}|^q. \qquad (11)\end{aligned}$$

We estimate the partition function as the power-law exponent of the variation of $\widehat{S}_j(q)$ versus scale 2^j. In practice, we use a linear regression of $\log_2\widehat{S}_j(q)$ versus j between scales j_1 and j_2

$$\widehat{T}(q) := \sum_{j=j_1}^{j_2} a_j \,\log_2\, \widehat{S}_j(q). \qquad (12)$$

[1] Since the wavelet coefficients are Gaussian, $\widehat{S}_j(q)$ converges only for $q>-1$.

The regression weights a_j must conform to the two conditions $\sum_j a_j = 0$ and $\sum_j j\, a_j = 1$ [4]. Using the simple form that the Legendre transform takes for differentiable functions such as T, we can estimate $f_{\mathrm{L}}(\alpha)$ through a local slope estimation of $\widehat{T}(q)$

$$\left\{ \begin{array}{rcl} \widehat{\alpha}(q_i) & = & [\widehat{T}(q_{i+1}) - \widehat{T}(q_i)]/q_0, \quad q_i = i q_0 \\ \widehat{f_{\mathrm{L}}}(\alpha(q_i)) & = & q_i\, \widehat{\alpha}(q_i) - \widehat{T}(q_i). \end{array} \right. \tag{13}$$

3.2 Statistics of the estimator for fBm

While random data is typically involved in applications of multifractal spectrum estimation, the statistics of the estimators have not previously been derived. In this section we take a first step in this direction by deriving approximate first and second order statistics for the wavelet-based multifractal spectrum of fBm. The analysis of fBm is a good starting point, since its trivial spectrum is actually nontrivial to estimate, due to *(i)* diverging moments for $q < -1$ and *(ii)* a linear partition function for $q > -1$. Testing a multifractal spectrum estimator with an fBm process is akin to testing a Fourier spectrum estimator with a sinusoidal process. In the following, recall that we assume that the fBm wavelet coefficients are independent. Our results should be compared with similar ones in [4].

Preliminaries: As defined in (11), $\widehat{S}_j(q)$ is the unbiased sample mean estimator for the random variable $|d_{j,k}|^q$ which, using P2, has, for $q > -1$, probability density function $p(u) := \frac{\sqrt{2}}{\sqrt{\pi}\sigma_j q}\, u^{\frac{1}{q}-1} \exp\left(-\frac{u^{2/q}}{2\sigma_j^2}\right)$, with finite mean and variance. Applying the Central Limit Theorem, we have

$$\widehat{S}_j(q) \to \mathbb{E}|d_{j,k}|^q \quad \text{as } N \to \infty. \tag{14}$$

More precisely, using P4, we have that $\widehat{S}_j(q)$ is *asymptotically normal* (AN) with mean $\mu = 2^{jT(q)}\, \mathbb{E}|d_{0,0}|^q$ and variance $\sigma_{j,q}^2 = \frac{2^{2jT(q)}\, \mathrm{Var}\, |d_{0,0}|^q}{2^{-j}N}$ [16]. It is clear that *(i)* μ is independent of the sample size N and *(ii)* $\sigma_{j,q}^2 \to 0$ as $N \to \infty$. Therefore, $\log_2 \widehat{S}_j(q)$ is also AN [16, p. 118] with

$$\begin{array}{rcl} \mathbb{E} \log_2 \widehat{S}_j(q) & = & jT(q) + \log_2 \mathbb{E}|d_{0,0}|^q, \\ \mathrm{Var}\, \log_2 \widehat{S}_j(q) & = & \frac{\log_2^2 e}{2^{-j}N} \frac{\mathrm{Var}\, |d_{0,0}|^q}{\mathbb{E}^2 |d_{0,0}|^q}. \end{array} \tag{15}$$

The estimator (12) for the partition function is a linear combination of (independent) AN random variables. From the constraints imposed on the weights $\{a_j\}$, the following statistics of $\widehat{T}(q)$ are straightforward to derive [4]:

$$\begin{array}{rcl} \mathbb{E}\, \widehat{T}(q) & = & T(q) \\ \mathrm{Var}\, \widehat{T}(q) & = & \frac{\log_2^2 e}{N} \left(\sqrt{\pi} \frac{\Gamma\left(q+\frac{1}{2}\right)}{\Gamma^2\left(\frac{q+1}{2}\right)} - 1 \right) \sum_j a_j^2\, 2^j. \end{array} \tag{16}$$

Thus, $\widehat{T}(q)$ is (asymptotically) unbiased. However, for finite sample sizes $N < \infty$, $\log_2 \widehat{S}_j(q)$ behaves more like $\mathbb{E} \log_2 \widehat{S}_j(q) = j\widehat{T}(q) + g(j)$, with $\lim_{N2^{-j} \to \infty} g(j)/j = 0$. In practice, the scale-dependent bias $g(j)$ introduces a corresponding bias into $\widehat{T}(q)$ (see Figure 1(a)).

(a)
(b)

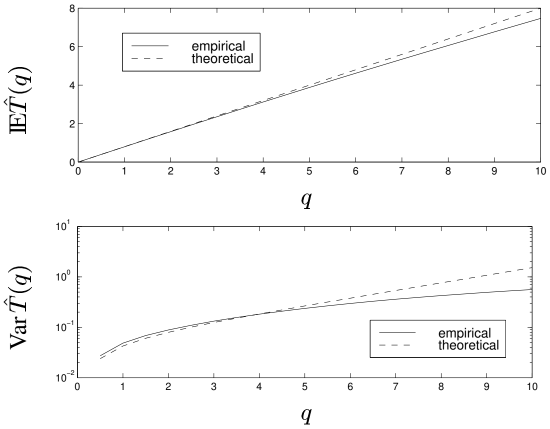

Figure 1. Statistics of the estimator $\widehat{T}(q)$ versus q. (a) $\mathbb{E}\widehat{T}(q)$; (b) log Var $\widehat{T}(q)$. Numerical results based on 1000 realizations of an fBm (exact Cholesky synthesis algorithm) with $H = 0.8$ and $N = 1024$ and a Daubechies wavelet with three vanishing moments.

Bias: Using the linearity of estimator (13), the first moments of $\widehat{\alpha}$ and $\widehat{f_{\mathrm{L}}}(\alpha)$ read (for $q > -1$ and $N \to \infty$)

$$\mathbb{E}\widehat{\alpha}(q_i) = q_0^{-1} \left(\mathbb{E}\, \widehat{T}(q_{i+1}) - \mathbb{E}\, \widehat{T}(q_i) \right) = H, \tag{17}$$

$$\mathbb{E}\widehat{f_{\mathrm{L}}}(\alpha(q_i)) = 0, \quad q_i > -1. \tag{18}$$

While asymptotically unbiased, the finite-sample bias in $\widehat{T}(q)$ carries over into $\widehat{\alpha}$ and $\widehat{f_{\mathrm{L}}}(\alpha)$, with the bias increasing with q (see Figure 2(a)). This can be explained by the rate of convergence of the sample moment estimators used in (11). For $q = 1$, the Berry-Esséen theorem [16, p. 33] asserts an $O(N^{-1/2})$ rate for the convergence of the normal approximation error. For $q = 2$, even though this $O(N^{-1/2})$ rate (found via consideration of $\widehat{S}_j(2)$ as a $U-$statistic [16, p. 193]) continues to hold, the asymptotic constant is larger.

Variance: We now estimate the variance of $\widehat{\alpha}(q_i)$ under the independence hypothesis for the fBm wavelet coefficients and the resulting asymptotic normal distributions ($N \to \infty$). A straightforward calculation yields

$$q_0^2\, \mathrm{Var}\, \widehat{\alpha}(q_i) = \mathrm{Var}\, \widehat{T}(q_{i+1}) + \mathrm{Var}\, \widehat{T}(q_i) - 2\, \mathrm{cov}\left(\widehat{T}(q_{i+1}), \widehat{T}(q_i)\right) \tag{19}$$

and

$$\mathrm{cov}\left(\widehat{T}(q_{i+1}), \widehat{T}(q_i)\right) = \sum_{j=j_1}^{j_2} a_j^2\, \mathrm{cov}\left(\log_2 \widehat{S}_j(q_{i+1}), \log_2 \widehat{S}_j(q_i)\right). \tag{20}$$

The estimates $\widehat{T}(q_i)$ are correlated due to the correlations in the $\widehat{S}_j(q_i)$. Using a moment estimation theorem [16, p. 68], we know that the variables $\widehat{S}_j(q_i)$ and $\widehat{S}_j(q_{i+1})$ are jointly Gaussian with covariance matrix elements

$$\begin{aligned}\sigma_{i,i+1} &= \mathbb{E}\widehat{S}_j(q_i+q_{i+1}) - \mathbb{E}\widehat{S}_j(q_i)\,\mathbb{E}\widehat{S}_j(q_{i+1}) \\ &= \frac{2^j}{N} 2^{j(q_i+q_{i+1})H}\left(\mathbb{E}|d_{0,0}|^{q_i+q_{i+1}} - \mathbb{E}|d_{0,0}|^{q_i}\,\mathbb{E}|d_{0,0}|^{q_{i+1}}\right).\end{aligned} \tag{21}$$

Using again a multivariate generalization of the asymptotic theorem on functions of AN random variables [16, p. 122], the covariance between $\log_2 \widehat{S}_j(q_i)$ and $\log_2 \widehat{S}_j(q_{i+1})$ can be written as $\frac{\log_2^2 e\, 2^j}{N}\left(\frac{\mathbb{E}|d_{0,0}|^{q_i+q_{i+1}}}{\mathbb{E}|d_{0,0}|^{q_i}\,\mathbb{E}|d_{0,0}|^{q_{i+1}}} - 1\right)$. Finally, we have

$$\begin{aligned}\operatorname{Var}\hat{\alpha}(q_i) &= \frac{\sqrt{\pi}\log_2^2 e}{N q_0^2}\sum_{j=j_1}^{j_2} a_j^2\, 2^j \\ &\times\left(\frac{\Gamma\left(q_i+\frac{1}{2}\right)}{\Gamma^2\left(\frac{q_i+1}{2}\right)} + \frac{\Gamma\left(q_{i+1}+\frac{1}{2}\right)}{\Gamma^2\left(\frac{q_{i+1}+1}{2}\right)} - \frac{2\Gamma\left(\frac{q_i+q_{i+1}+1}{2}\right)}{\Gamma\left(\frac{q_i+1}{2}\right)\Gamma\left(\frac{q_{i+1}+1}{2}\right)}\right).\end{aligned} \tag{22}$$

Figure 2(b) demonstrates experimentally that $\operatorname{Var}\hat{\alpha}(q)$ does not vary significantly with the sampling rate q_0 (defined in (13)): the prefactor q_0^{-2} in (22) is balanced by the increasing correlation between $\log_2 \widehat{S}_j(q_i)$ and $\log_2 \widehat{S}_j(q_{i+1})$ when $q_0 \to 0$. In contrast to the simplified estimator $\widehat{a}(q) = \frac{1}{q}\widehat{T}(q)$ proposed in [4], the estimator $\widehat{\alpha}(q)$ from (13) has a higher variance. However, $\widehat{a}(q)$ is not fit for the recovery of the multifractal spectrum from a Legendre transform for at least two strong reasons. First, when studying processes other than fBm, partition functions will generally not be linear but strictly concave, in which case the simplified estimator is not appropriate. Second, even for fBm the simplified estimations of H will depend on q due to bias (see Figure 1(a)). Using $\widehat{a}(q)$ instead of $\widehat{\alpha}(q)$ in (13) the Legendre transform yields $\widehat{f_{\mathrm{L}}}(\alpha(q)) = 0\ \forall \widehat{a}(q)$, hence a flat spectrum. Such a spectrum could very well be mistaken for the one of a generalized Weierstrass multifractional process [8], a process with indeed a varying H_t and a flat spectrum. Thus, the simplified estimator is unreliable for distinguishing between monofractal and multifractal behavior. In contrast, the estimator (13) shows a significant local maximum $\widehat{f_{\mathrm{L}}}(\alpha) = 0$ at $\widehat{\alpha}(q) = H$ for monofractal processes such as fBm (see Figure 3) and a flat spectrum for the generalized Weierstrass multifractional process (see Figure 4).

3.3 Further caveats

The case $q < -1$: When $q < -1$, our Gaussian assumptions fail. Convergence theorems on iid infinitely divisible laws state that properly normalized sums of iid

(a)

(b)

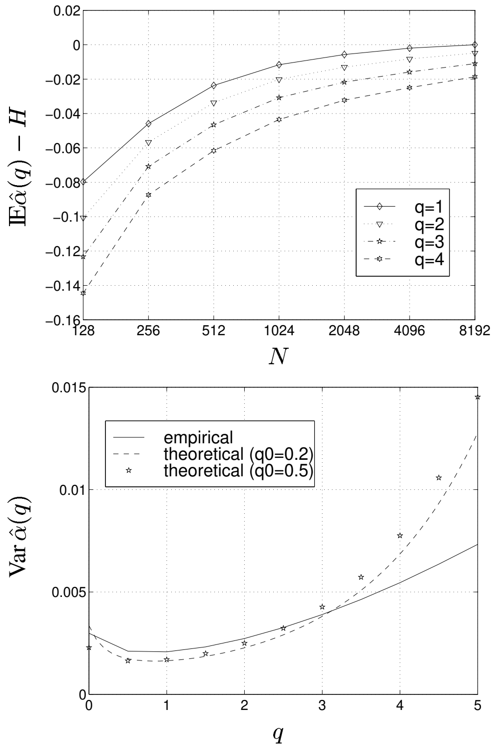

Figure 2. Statistics of $\widehat{\alpha}(q)$. (a) Bias: $\widehat{\alpha}(q)$ is asymptotically unbiased. We plot the evolution of $H - \mathbb{E}\widehat{\alpha}(q)$ versus the sample size N for different values of exponent q. (b) Variance: We plot $\operatorname{Var}\widehat{\alpha}(q_i)$ versus q_i for $N = 1024$ and for two values of q_0 ($*$ and dashed line). Experimental conditions are identical to those of Figure 1.

$|d_{j,k}|^q$ converge towards a stable law [7] with stability parameter $\gamma = -1/q$

$$p(u) = \frac{-\sqrt{2}}{\sqrt{\pi}\sigma_j q}\, u^{\frac{1}{q}-1}\, \exp\left(-\frac{u^{2/q}}{2\sigma_j^2}\right). \tag{23}$$

For $-2 \leq 1/q - 1 < -1$ and for all $r > -1/q$, $\mathbb{E}u^r$ is infinite. An empirical stability test allows us to set $\widehat{S}_j(q) = \infty$ whenever the series $|d_{j,k}|^q$ follows (approximately) a positive stable distribution. The experimental results in Table 1 correspond to the estimation of γ (using the Koutrouvelis procedure [11]) from one scale band of fBm wavelet coefficients.

Adaptive linear regression: The standard linear regression of (12) is optimal only for Gaussian random variables. In the finite sample, non-Gaussian case, we could conceivably compute the probability density function $\widehat{S}_j(q)$ and adjust the regression parameters $\{a_j\}$ to minimize some error measure in the partition function estimate (12).

4 Conclusions

In this paper we have derived, in the simple case of the fBm, the first and second order asymptotic statistics of

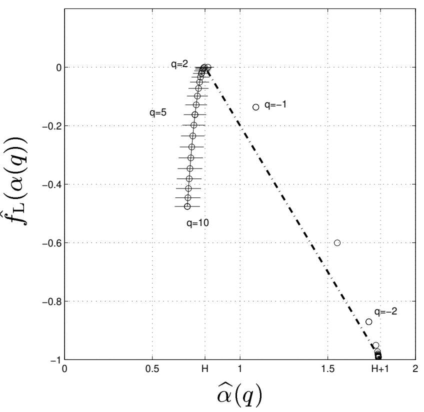

Figure 3. Empirical statistics on $\widehat{f_L}(\alpha(q))$ plotted versus $\widehat{\alpha}(q))$ for fBm. The dashed dot line corresponds to the theoretical Legendre spectrum. The error bars denote the standard deviation on the estimates $\widehat{\alpha}(q)$. Experimental conditions are identical to those of Figure 1.

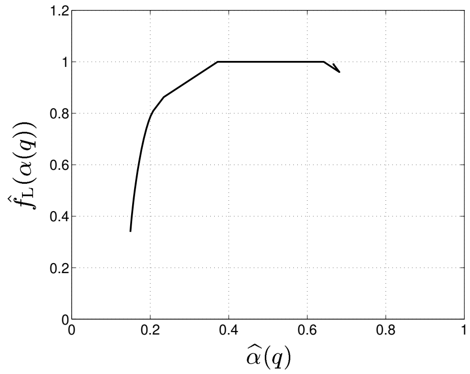

Figure 4. Wavelet-based Legendre spectrum estimator (13) averaged over 100 independent realizations of a generalized Weierstrass process [8] $W(t) := \sum_k \lambda^{-kH_t} \sin(\lambda^k t + \phi_k)$ with ϕ_k uniform random variables on $[0, \pi[$. The Hölder function H_t grows linearly from $H_0 = 0.2$ to $H_1 = 0.8$.

Table 1. Koutrouvelis stability test [11] applied to the series $\{|d_{j=1,k}|^q\}$ obtained from one scale band ($j = 1$) of the wavelet transform of an fBm. For $q < -1$, $|d_{j=1,k}|^q$ is asymptotically stable distributed with stability parameter $\gamma = -1/q$.

q	-10	-5	-3	-1	1
$-1/q$	0.1	0.2	0.3	1	2
estimated γ	0.125	0.215	0.345	0.75	1.81

a wavelet-based Legendre multifractal spectrum estimator. Our results indicate that because of its decorrelating power, the wavelet transform is well adapted to estimating moment generating functions. In addition to providing confidence intervals on the multifractal spectrum, the statistics could be employed to construct an approximate hypothesis test for the validity of an fBm model in a given situation.

Our ongoing research focuses on extending the statistical calculations to the general multifractal case (going beyond the work of [1, 4]), dealing with diverging moments using the Koutrouvelis stability test, and developing adaptive weighted linear regressions for non-Gaussian data.[2]

References

[1] P. Abry, P. Gonçalvès and P. Flandrin, Wavelets, spectrum analysis and $1/f$ processes, In *Lectures Notes in Statistics: Wavelets and Statistics*, (A. Antoniadis, Ed.). 1995.

[2] E. Bacry, J. Muzy, and A. Arneodo, Singularity spectrum of fractal signals from wavelet analysis: Exact results, *J. Stat. Phys.*, 70:635–674, 1993.

[2]Thanks to Patrice Abry for providing us with the manuscript [4].

[3] I. Daubechies, *Ten Lectures on Wavelets*, SIAM, 1992.

[4] L. Delbeke and P. Abry, Wavelet-based estimators for the self-similarity parameter of fractional Brownian motion, Submitted to *Appl. Comp. Harm. Anal.*, 1998.

[5] R. Ellis, Large deviations for a general class of random vectors, *Ann. Prob.*, 12:1–12, 1984.

[6] P. Flandrin, Wavelet analysis and synthesis of fractional Brownian motion, *IEEE Trans. Info. Theory*, 38:910–917, 1992.

[7] B.V. Gnedenko and A.N. Kolmogorov, Limit distributions for sums of independent random variables, *Addison-Wesley*, 1968.

[8] P. Gonçalvès and P. Flandrin, Scaling exponents estimation from time-scale energy distributions, *IEEE ICASSP*, San Francisco, 1992.

[9] S. Jaffard, Pointwise smoothness, two-microlocalization and wavelet coefficients, *Publications Mathematiques*, 35:155–168, 1991.

[10] S. Jaffard, Local behavior of Riemann's function, *Contemporary Mathematics*, 189:287–307, 1995.

[11] I.A. Koutrouvelis, Regression type estimation of the parameters of stable laws, *Am. Stat. Assoc.*, 75:918–928, 1980.

[12] W. Leland, M. Taqqu, W. Willinger, and D. Wilson, On the self-similar nature of Ethernet traffic, *IEEE/ACM Trans. Networking*, pp. 1–15, 1994.

[13] B. B. Mandelbrot, Intermittent turbulence in self similar cascades: Divergence of high moments and dimension of the carrier, *J. Fluid. Mech.*, 62:331, 1974.

[14] R. Riedi, M. S. Crouse, V. Ribeiro, and R. G. Baraniuk, A multifractal wavelet model with application to TCP network traffic, *IEEE Trans. Info. Theory* (special issue on multiscale statistical signal analysis and its applications), 1999.

[15] R. H. Riedi, Multifractal processes, *Stoch. Proc. Appl.*, preprint, 1999.

[16] R. Serfling, *Approximation theorems of Mathematical Statistics*, Wiley, 1980.